

# Simulation of polycyclic aromatic hydrocarbon remobilization in typical active regions of river system under hydrodynamic conditions

Lili Wang · Zhifeng Yang

Received: 26 May 2010 / Accepted: 12 August 2010 / Published online: 25 August 2010  
© Springer-Verlag 2010

## Abstract

**Purpose** In an aquatic environment, hydrodynamic condition is a ubiquitous natural process, and the contaminated sediments will act as a potential pollution source once they are remobilized into the overlying water. In this study, remobilization behavior of polycyclic aromatic hydrocarbons (PAHs) under simulated hydrodynamic conditions was studied. Additionally, an adjusted prediction model with additive consideration of surface properties was developed to exhibit the distribution of PAHs in hydrodynamic system.

**Materials and methods** An improved syntonic turbulence-simulation device (TSD) was used to simulate hydrodynamic conditions. Two sediments from the Yellow River Delta (YRD) and the intersection of Yangtze and Hanjiang River (YHR), respectively, were used to represent variations in organic carbon contents and sediment surface characteristics. Five PAHs including acenaphthene (Ace), fluorine (Flu), phenanthrene (Phe), fluoranthene (Fla), and pyrene (Pyr) were selected as the target compounds in this study.

**Results and discussion**  $\sum$ PAH concentrations in particles on volume normalization increased 74.1% and 18.5% for the YRD and YHR samples, respectively, and the same increasing trend was observed for individual PAHs. On mass weight basis,  $\sum$ PAHs were observed to decrease for both the YRD (from 2,039.5 to 1,149.7 ngg<sup>-1</sup>) and YHR (4,222.7 ngg<sup>-1</sup> to 2,914.2 ngg<sup>-1</sup>) samples. Interestingly, concerning the different

heights of the TSD, the YRD-associated PAHs showed an opposite behavior comparing with the YHR-bound PAHs.

**Conclusions** The remobilization of less contaminated, larger-size particles was found to skew the PAH concentration downward, which resulted in the opposite PAH behaviors of the YRD and YHR samples. The distribution of PAHs between solid and liquid phases was affected by both organic carbon contents and surface areas of the remobilized sediments.

**Keywords** Hydrodynamic conditions · Polycyclic aromatic hydrocarbons · Prediction model · Remobilization · Turbulence-simulation device

## 1 Introduction

Polycyclic aromatic hydrocarbons (PAHs), originated mainly from incomplete combustion of fossil fuels and biomass, are ubiquitous throughout the environment such as air, water, soil, sediments, plants, and animals (Lee et al. 2005; Niu et al. 2007; Stout et al. 2004; Troisi and Borjesson 2005; Wang et al. 2010). Due to their toxic effects on organisms, some of the PAHs have been studied widely all over the world (Chen et al. 2001; Kim and Weber 2005; Long and Niu 2007; Niu et al. 2003, 2004; Niu and Yu 2004; Wang et al. 2007, 2009b). As one of the major sinks of PAH contamination, aquatic environmental system has received much attention for PAH investigations (Tao et al. 2003; Wang et al. 2009c). Owing to their high hydrophobicity, PAHs have a great tendency to associate with particulate materials and finally deposit in underlying sediments (Chiu et al. 1998; Tolosa et al. 2004). Consequently, sediments act as an important sink for these hydrophobic compounds (Colombo et al. 2006; Urban et al. 2010). In the aquatic

---

Responsible editor: Jan Schwarzbauer

---

L. Wang · Z. Yang (✉)  
State Key Laboratory of Water Environment Simulation,  
School of Environment, Beijing Normal University,  
Beijing 100875, People's Republic of China  
e-mail: zfyang@bnu.edu.cn

environment, hydrodynamic condition is a ubiquitous natural process especially for the active regions of river system such as estuary areas and river intersections. Once remobilized into the overlying water under hydrodynamic conditions, the contaminated sediments will act as a potential contamination source to the water column (Feng et al. 2007b; Latimer et al. 1999; Smit et al. 2010; van der Heijden and Jonker 2009).

Investigations on the remobilization and behavior of contaminants under hydrodynamic conditions have been an issue for several years (Alkhatib and Weigand 2002; de Vicente et al. 2010; Hedman et al. 2009; Latimer et al. 1999; Rockne et al. 2002; van der Heijden and Jonker 2009). However, the contaminant changes during the remobilization process have not been clearly understood. In remobilization events, the contaminants might be sorbed to the resuspended material and removed from water column, however, they might also be released to the aqueous phase, and their availability in solution was therefore increased (de Vicente et al. 2010). Moreover, previous studies revealed that variations of dissolved PAHs in the overlying water were not uniform on account of different sediment compositions and complicated phase changes (Latimer et al. 1999; Yang et al. 2008). Thus, further investigations of the contaminant distribution in response to the hydrodynamic conditions are needed to provide a better understanding of their remobilization behavior.

Although the factors affecting the behavior of contaminants during remobilization events have been studied by some researchers, few prediction models for describing the contaminant distribution in hydrodynamic system have been developed. So far, organic matter normalized partition coefficient ( $K_{OC}$ ) was commonly used for estimating the PAH distribution between solid and liquid phases. Wang et al. (2009a) investigated the role of grain size in the remobilization of phenanthrene (Phe), and attributed the influence of grain size to the effect of organic carbon content in sediments. Accordingly, a sorption dynamic model was built based on the linear isotherm expression. Similarly, the affecting mechanism of PAH distribution between the dissolved and particulate phases is also considered to be mainly due to the linear partition into organic carbon by other researchers. Prediction models were accordingly developed, and the differences between measured and predicted values were supposed to be due to the presence of other active sorbents in sediment (Feng et al. 2007b; Latimer et al. 1999). However, as sediment is a multi-component mixture, its sorption mechanisms cannot be distinctly determined by a single partition hypothesis (van der Heijden and Jonker 2009; Wang et al. 2008). In addition, under hydrodynamic conditions, particle collisions occurring during remobilization altered the size and surface areas of the suspended solid (DePinto et al. 1994).

Thus, further work is needed to develop a regulating prediction model by giving consideration to the surface properties of remobilized sediments.

The aim of the present study was to investigate the distribution of PAHs between the solid and liquid phases in response to the turbulence energy and remobilized sediment characteristics under hydrodynamic conditions. By applying an improved syntonetic turbulence-simulation device (TSD), two sediments from different active regions of river system were remobilized under two different turbulence energies. In addition, a prediction model for describing the PAH distribution in hydrodynamic system was developed from the view of hydrodynamic conditions.

## 2 Materials and methods

### 2.1 Sample collection

Two active regions of river system were chosen as sediment sample collection sites. One is located at the land–ocean interaction region of the Yellow River Delta (YRD), and the other one is at the intersection of the Yangtze River and Hanjiang River (YHR). Top 10-cm surface sediments were taken using a Van Veen stainless steel grab sampler (Eijkelamp, Netherlands). After collection, the samples were passed through a 500- $\mu\text{m}$  mesh sieve to remove macrofauna. The sediments were covered with sampling water and kept at 4°C in the dark prior to tests.

### 2.2 Chemicals

Acenaphthene (Ace), fluorine (Flu), phenanthrene (Phe), fluoranthene (Fla), and pyrene (Pyr) were selected as the target PAHs in this study. The working standard solutions were prepared by diluting appropriate volumes of the standard mixture (PAH-Mix 9, 100  $\text{ng}\mu\text{L}^{-1}$  in acetonitrile, Germany) with methanol. The background water was composed of 1-mM  $\text{CaCl}_2$  and some of 100- $\text{mg}\text{L}^{-1}$   $\text{NaN}_3$  in order to make the aquatic environment condition close to natural freshwater. All solutions were prepared using distilled water that was passed through a MilliQ UV-plus water purification system (Millipore, Bedford, MA, USA) with a specific resistivity of 18.2  $\text{M}\Omega\text{cm}$ .

### 2.3 Hydrodynamic experiments

An improved syntonetic turbulence-simulation device (TSD) was employed for simulating the natural aquatic environment and performing hydrodynamic experiments. The TSD was described elsewhere (Wang et al. 2009a). Briefly, the improved TSD consists of a vertical acrylic cylinder ( $\Phi=25$  cm,  $h=60$  cm) and a set of oscillating vibratory

grids driven by a variable speed motor which controlled the turbulence energy. As the turbulated particles distributed relatively evenly under high turbulence energies in the TSD, weaker hydrodynamic conditions were used in this study to provide insight into the sediment properties in each layer affecting the PAH behavior. The perforated grids were driven by variable speed motor with 70 and 100 rpm, which was mentioned as low energy (L energy) and high energy (H energy), respectively.

For dynamic testing, about 20 L of background water and appropriate amount of sediments (100 g for the YHA sediment and 150 g for the YRD sediment, respectively) were added to the cylinder and kept static for 48 h. The cylinder was positioned to the TSD unit, and the perforated grid was performed with the vertical amplitude of 3.2 cm, ranging between 5.0 and 8.2 cm above the sediment surface. After a 24-h process of oscillating turbulence, 1 L of samples was collected from the top, middle, and bottom sample ports on the device, respectively. After being centrifuged at 5,000 rpm for 20 min, the sediments were air-dried, and their physicochemical characteristics were analyzed.

By using a Liquid TOC analyzer (Elementar, Germany), total organic carbon content ( $f_{oc}$ ) of each sediment sample was determined. Moreover,  $N_2$ -surface area ( $S_A$ ) was measured by ASAP2010 (Micromeritics, America).

#### 2.4 Analytical methods

In order to evaluate the behavior of PAHs under hydrodynamic conditions, samples of different phases were measured for quantifying the PAH content. Filtered water samples were extracted with dichloromethane. The aqueous extracts were then reduced to a volume of 1–2 mL, subject to a solvent exchange to methanol, concentrated to 1.0 mL by the rotary evaporator prior to HPLC analysis. The suspended particulate matter (SPM) samples separated by pre-combusted glass fiber filters (0.45  $\mu\text{m}$  effective pore sizes, Beijing Shenghe Membrane Science and Technology Co., China) were freeze-dried until constant weights were maintained. SPM samples as well as sediments were mixed with 30-mL hexane/acetone mixture (1:1,  $v/v$ ) and left to settle overnight. The advanced PAH quantifying analysis was as demonstrated in our previous study (Wang et al. 2008).

#### 2.5 Quality control

Before the onset of the extraction and analysis program, PAH standard mixture was spiked with water and solid samples for the recovery experiments. The spiked samples were extracted, purified, and analyzed in the same way as normal samples. The results of recovery for the five PAHs were more than 60%. The relative standard deviations of

the mass balance determination experiments were less than 10%. Blank experimental results displayed that the effect of both device wall sorption and PAH volatilization was less than 3.2%. Under analytical condition, detection limits for the five PAHs ranged from 0.87 to 7.12  $\text{ngL}^{-1}$  for water samples and from 0.34 to 3.06  $\text{ngg}^{-1}$  for solid samples.

### 3 Results and discussion

#### 3.1 PAH sequestration correlated with sediment characteristics

##### 3.1.1 Mass-normalized PAH sequestration

The variations of PAH concentrations in remobilized particle for YRD and YHR on mass basis are exhibited in Fig. 1. As the turbulence energy increases,  $\Sigma\text{PAH}$  concentrations normalized by mass weight were observed to decrease for both the YRD (from 2,039.5 to 1,149.7  $\text{ngg}^{-1}$ ) and YHR (4,222.7  $\text{ngg}^{-1}$  to 2,914.2  $\text{ngg}^{-1}$ ) samples. This concentration trend was also found for individual PAHs (Table 1). This phenomenon is considered to be attributed to the turbulence of larger size sediments at higher turbulence energy. In the previous study, the median diameters of sediments under designed dynamic conditions in the simulation device were found to increase dramatically with the increase of turbulent energy, from 5.1 to 17.3  $\mu\text{m}$  at different turbulence energies (Wang et al. 2009a). Accordingly, the size of particles was larger under higher turbulence energy compared with the situation under lower turbulence energy. Many studies have investigated that the grain size distribution acts as an important variable which correlated well with the quantity of PAHs (Ahrens and Depree 2004; Lee et al. 2005; Wang et al. 2001). Larger size sediment fractions were often

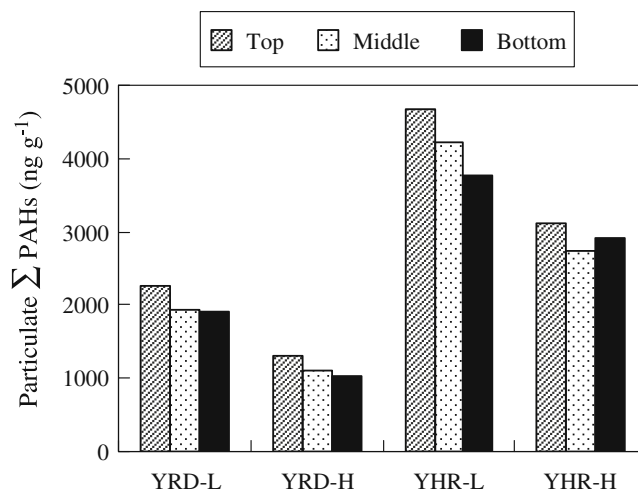


**Fig. 1** Mass loading PAHs on remobilized particles normalized to dry weight

**Table 1** Average mass loading of individual PAHs on remobilized sediments under different turbulence energies (ngg<sup>-1</sup>, dw)

Sediments	Turbulence	Ace	Flu	Phe	Fla	Pyr
YRD	Low energy	120.07	95.22	525.02	690.90	608.30
	High energy	60.50	48.17	318.53	394.00	328.53
YHR	Low energy	152.54	393.15	766.97	1,628.41	1,281.58
	High energy	117.02	63.37	650.92	1,097.50	985.39

observed to contain relatively low PAH concentrations (Wang et al. 2009a). The less contaminated, larger size sediment fractions are considered to skew the compound concentration downward and dilute the contaminants. The similar results have been observed for PAHs and PCBs by other researchers during resuspension events (Feng et al. 2007b; Latimer et al. 1999).

The second explanation for this phenomenon was the redistribution of PAHs to water column. As the turbulence energy increased, the particle aggregation was intensified which could be implied by the result of surface area analysis for the remobilized sediments in Table 2. The loss of adsorption sites on particles results in the transfer of contaminants from particle flocs to water phase which contributes to the decreasing of contaminant on particles under higher turbulence energy (Alkhatib and Weigand 2002).

3.1.2 Volume-normalized PAH sequestration

Total suspended solids (TSS) for each TSD run were measured and were found to increase with the increasing turbulence energy (see Table 2). As the height changed from bottom to top, TSS values were observed to decrease for both YHR and YRD samples. This phenomenon indicates that the hydrodynamic condition plays an important role in the distribution of sediment concentration in the aquatic environment.

On the basis of TSS and mass loading PAH values, volume-normalized concentrations of PAHs were calculated and observed to generally increase with the increasing of turbulent energy (Fig. 2). On average, the ΣPAH concentration increased from 456.0 ngL<sup>-1</sup> at lower turbulent energy to 793.9 ngL<sup>-1</sup> at higher energy for YRD samples. In the case of YHR solids, the corresponding ΣPAH

concentration increased from 1,164.1 to 1,378.9 ngL<sup>-1</sup>. Referring to individual PAHs, the same trend was observed (see Fig. 2). Concentrations of YRD-associated PAHs increased as much as 38.9% to 85.8%, and the YHR samples showed less increase, from 8.4% to 59.3%. These results corresponded to the variation of TSS amount under different turbulence energies for different sediments (see Table 2). YRD samples exhibited a relatively greater response to the turbulence energy, and it showed more significant TSS increase than the YHR samples. Moreover, according to the results of PAH concentration, the turbulence events were found to remobilize significant amounts of PAHs into the water column, implying that the water quality criteria could be exceeded as the result of turbulence although they may be under the safety standard in static condition. Accordingly, sediment remobilization could cause periodic exposure of aquatic organisms with PAHs and results in subsequent adverse effects. Other researchers have also noted that the turbulence condition could act as a potential pollution source to water column (Alkhatib and Castor 2000; Feng et al. 2007b; Martino et al. 2002; Saulnier and Mucci 2000).

Lower-aqueous solubility (S<sub>w</sub>) PAHs (i.e., Phe, Fla, and Pyr) were found to be dominant components on the remobilized particles under both low and high turbulent energies. Phe, Fla, and Pyr accounted for more than 80% of the ΣPAH concentration, which was supposed to be on account of the common distribution of four-ring PAH fractions in the Yellow River Delta (Yang et al. 2009) and the intersection of Yangtze and Hanjiang River (Feng et al. 2007a). The similar phenomenon was also observed by Feng et al. (2007b) who investigated the resuspension event for sediments from the intersection of Yangtze and Hanjiang River by using a particle entrainment simulator.

**Table 2** Particle and aqueous properties under different turbulence energies

Parameters	Sites	Bulk	Low energy			High energy		
			Top	Middle	Bottom	Top	Middle	Bottom
TSS <sup>a</sup>	YRD	–	160.0	204.3	226.3	659.3	706.7	712.4
	YHR	–	241.8	259.2	271.7	384.0	456.5	480.9
S <sub>A</sub> <sup>b</sup>	YRD	–	4.53	4.86	3.09	3.51	3.50	3.52
	YHR	–	9.00	8.36	8.68	7.33	7.44	7.19
f <sub>oc</sub> <sup>c</sup>	YRD	0.16	1.65	1.57	1.38	0.81	0.69	0.67
	YHR	1.00	2.16	2.04	2.14	1.77	1.63	1.50

(–) No data

<sup>a</sup> Total suspended solid (mgL<sup>-1</sup>)

<sup>b</sup> Surface area (m<sup>2</sup> g<sup>-1</sup>)

<sup>c</sup> Organic carbon content (%)

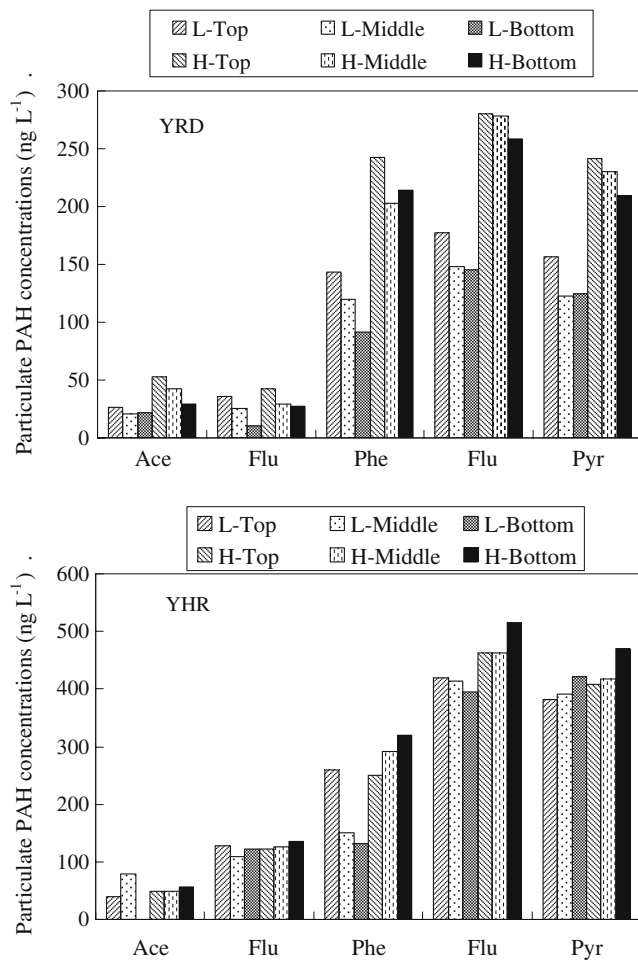


**Fig. 2** The concentration profiles on a volume normalized basis for PAHs versus applied shear during the study

Comparing the PAH concentrations at different heights (top, middle, and bottom), the YRD-associated PAHs showed a decreasing trend from the top to bottom layer in the TSD. However, the PAHs combined on YHR showed an opposite trend. According to the TSS values in Table 2, it can be seen that the TSS amounts at bottom layers were higher than the top layers. Accordingly, the PAH concentrations in the particles at the bottom should be greater. For the YRD samples, the increase in the amount of TSS at the bottom layer was not so large (see Table 2). Based on the textual considerations, the YRD particles had a greater proportion of larger size sediment than the YHR (median diameter,  $d_{50,YRD}=46.8 \mu\text{m}$ ;  $d_{50,YHR}=28.1 \mu\text{m}$ ), and these particles for YRD at the bottom of TSD skewed the concentration downward, additionally, it improved the results in Section 3.1.1.

### 3.2 Solid–water phase relationships

The dissolved fraction of PAHs in overlying water showed a decreasing trend as the turbulence energy increased for

both YRD (from 6.66 to 5.84  $\mu\text{g L}^{-1}$  on average) and YHR (from 5.82 to 4.81  $\mu\text{g L}^{-1}$  on average) samples. With regard to individual PAHs, Ace and Flu were observed to maintain relatively constant with the increasing turbulence energy. However, relatively lower- $S_w$  PAHs (i.e., Phe, Fla, and Pyr) presented a decreasing trend during the remobilization experiments.  $\Sigma\text{PAHs}$  in liquid phase is in accordance with the mass loading of  $\Sigma\text{PAHs}$ , as the result of dominant PAHs of Phe, Fla, and Pyr accounting for most of the PAH composition.

The apportioning of PAHs between solid and liquid phases is commonly depicted with the distribution coefficient ( $K_d$ ):

$$K_d = C_p / C_d \quad (1)$$

where  $C_p$  is the PAH concentration in the particle phase,  $\mu\text{g kg}^{-1}$ ;  $C_d$  is the concentration in dissolved phase,  $\mu\text{g L}^{-1}$ . The  $K_d$  values for individual PAHs on each height of the TSD were calculated and were found to be positively related to the organic content ( $f_{oc}$ ) of each particle sample ( $R=0.834\sim 0.988$ ). Accordingly, the  $K_d$  for PAHs in this study was

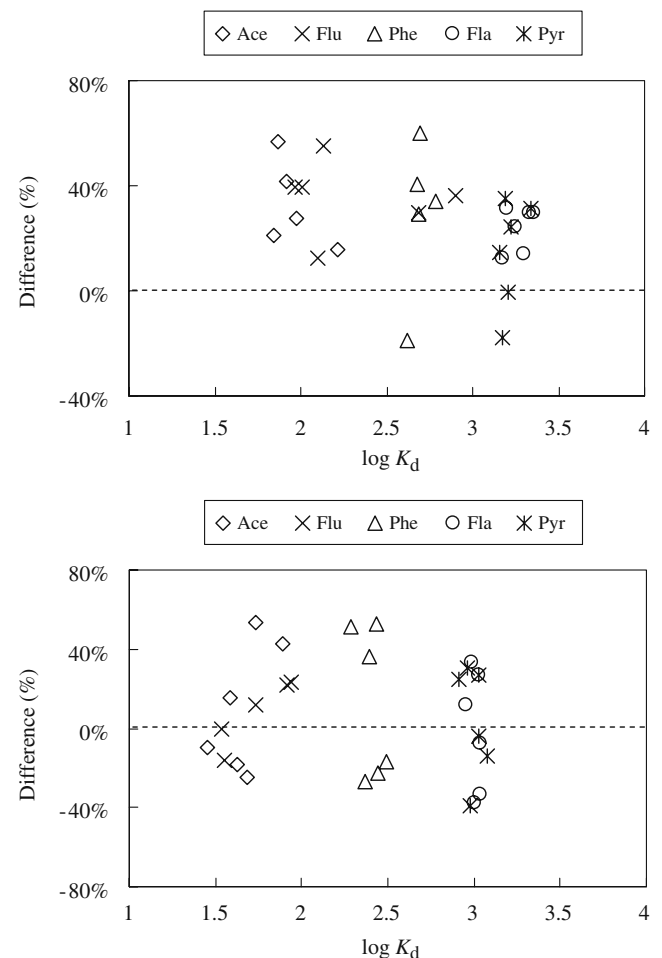


**Fig. 3** Percent difference between predicted and measured  $K_d$  values for each PAH during the remobilization event

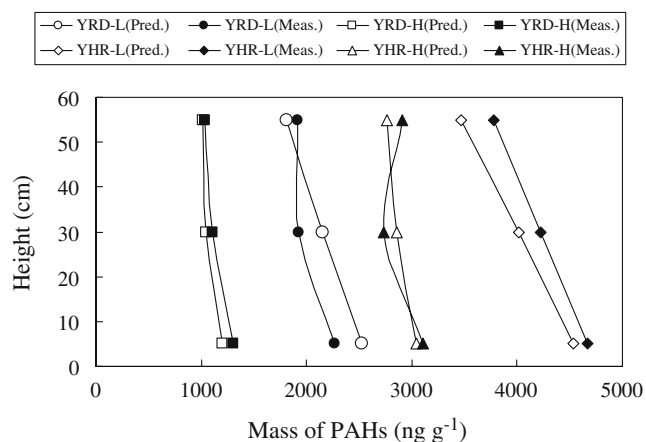


**Fig. 4** The vertical distribution of  $\Sigma$ PAHs on suspended particles under different hydrodynamic conditions

predicted from published  $K_{OC}$  values (Karickhoff et al. 1979) together with  $f_{oc}$  measured in remobilized particles using Eq. (2):

$$K_d = f_{oc}K_{OC} \tag{2}$$

According to Eq. (2), the predicted  $\log K_d$  values for all of measured PAHs were shown in Fig. 3. The  $f_{oc}$  was known to play an important role in the partition of PAHs onto particles. Accordingly, the predicted  $K_d$  values for PAHs should compare favorably with the measured coefficients. However, it appeared that for higher- $S_W$  PAHs (i.e., Ace and Flu), the measured amount of PAH was generally greater than the predicted values, especially for the YRD samples which had less  $f_{oc}$ . This could be due to the presence of another active sorbent besides organic carbon in the solid samples (Latimer et al. 1999). The same phenomenon was also found for Ace and Flu by Feng et al. (2007b), and the result was attributed to the sorption onto mineral surfaces which might be an additional means to elevate the  $K_d$  values. Other researchers also attributed the PAH sorption to both organic carbon partition and particle surface area adsorption (Allen-King et al. 2002; Joo et al. 2008; Pignatello et al. 2006; Rockne et al. 2002; Xing et al. 1996). The correlation between PAH concentrations and  $S_A$  for each remobilized particle sample was determined, and the results indicated a relatively high relationship coefficient ( $R=0.879\sim 0.924$ ). Accordingly, a sorption model giving consideration to the surface adsorption in addition to the organic carbon partition was employed based on the two-component model developed by Joo et al. (2008) for predicting the distribution coefficient of higher- $S_W$  PAHs:

$$K_d = K_{OC}f_{OC} + (1 - f_{OC})S_AK_S \tag{3}$$

where  $K_S$  is the surface area normalized distribution coefficient,  $Lm^{-2}$ .

The contributions of both  $f_{oc}$  and  $S_A$  to the overall sorption of compounds were included in Eq. (3). The  $K_S$  is

calculated by using the surface area values based on  $N_2$  adsorption. In general, all of the resulting  $K_S$  values for the nonpolar neutral organic compounds were on the order of  $10^{-5} Lm^{-2}$  (Joo et al. 2008). In this study,  $K_S=10^{-5} Lm^{-2}$  was used for calculating.  $S_A$  was multiplied by  $10^3$  to meet the unit of  $m^2kg^{-1}$ . With the adjusted model (3), all the differences between the measured and predicted  $K_d$  values for Ace and Flu were within 40%, suggesting relatively accurate predictions.

### 3.3 Prediction model

Based on the current results, a prediction model was developed for describing the PAH distribution in hydrodynamic system. Linear isotherm was employed to describe the partition behavior of lower- $S_W$  PAHs (i.e., Phe, Fla, and Pyr), and the adjusted distribution coefficient model was used to depict the sorption behavior of higher- $S_W$  PAHs (i.e., Ace and Flu). Combining the distribution coefficient expression and the law of mass conservation, a prediction model for determining the PAH distribution in the hydrodynamic system was developed and expressed as follows:

$$K_d = K_{OC}f_{OC} + (1 - f_{OC})S_AK_S \quad (\text{for Ace and Flu}) \tag{4}$$

$$K_{i,j} = K_{OC,j}f_{OC} \quad (\text{for Phe, Fla, and Pyr}) \tag{5}$$

$$q_{i,j} = K_{i,j}C_{e,j} \tag{6}$$

$$Q_i = \sum_{j=1}^5 q_{i,j}SS_i \tag{7}$$

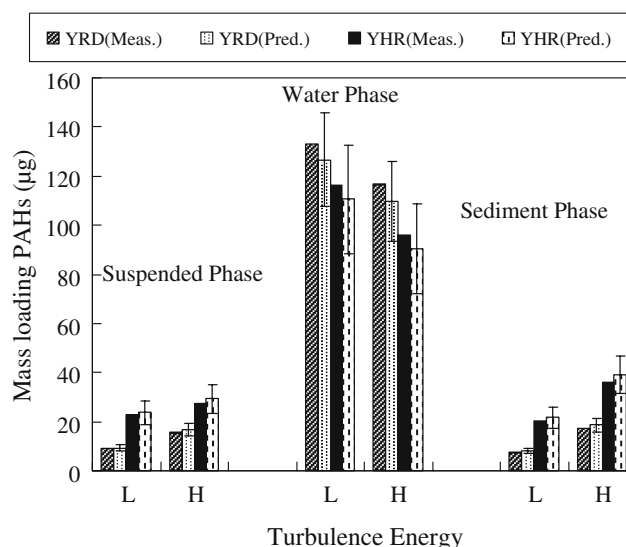


**Fig. 5** The distribution of  $\Sigma$ PAHs in three phases under different hydrodynamic conditions

$$Q = \sum_{i=1}^3 \sum_{j=1}^5 K_{i,j} C_{e,j} S S_i \quad (8)$$

$$S = N_0 - C_e V - Q \quad (9)$$

where  $K_{OC,j}$  is the  $K_{OC}$  value of  $j$ -individual PAH;  $K_{i,j}$  is the distribution coefficient of sediment with  $j$ -individual PAH in  $i$  layer;  $C_{e,j}$  stands for equilibrium aqueous-phase  $j$ -individual PAH concentration ( $\mu\text{gL}^{-1}$ );  $q_{i,j}$  stands for the amount of  $j$ -individual PAH sorbed per unit mass of sediment in  $i$  layer ( $\mu\text{gkg}^{-1}$ );  $Q_i$  is the mass of  $\Sigma$ PAHs in suspended phase in  $i$  layer ( $\mu\text{g}$ );  $Q$  is the mass of  $\Sigma$ PAHs in suspended phase ( $\mu\text{g}$ );  $S$  is the mass of  $\Sigma$ PAHs in sediment phase ( $\mu\text{g}$ );  $V$  stands for the water volume in turbulent device (L); and  $N_0$  is the total mass of  $\Sigma$ PAHs in turbulent device ( $\mu\text{g}$ ).

Based on Eqs. (4, 5, 6, 7, 8 and 9), the PAH mass loadings in three heights under different turbulence energies were calculated, and the results were compared with the experimental data in Fig. 4. In addition, the distribution of PAHs in liquid phase, suspended particles, and sediment phase was obtained and discussed based on the concentration of PAHs in aqueous phase (Fig. 5). The results showed that the predicted values were in good agreement with the experimental data (with the differences from 2.1% to 11.7%) in three phases under different hydrodynamic conditions. The prediction model was validated by PAH behavior acquired with two different hydrodynamic conditions and two sediment samples, and it provided information to predict the distribution of PAHs in hydrodynamic system.

#### 4 Conclusions

Significant amounts of particulate PAHs were introduced into the water column during the remobilization process of sediments. The concentrations of PAHs generally increase with the increasing of turbulent energy, from 456.0 to 793.9  $\text{ngL}^{-1}$  for YRD samples and from 1,164.1 to 1,378.9  $\text{ngL}^{-1}$  for YHR samples as the result of increasing suspended solids during the remobilization events. Comparing the PAH concentrations at different heights (top, middle, and bottom) of the TSD, the YRD-associated PAHs showed an opposite behavior to the YHR-bound PAHs due to the textual variation of the two sediments. On the basis of mass weight normalization,  $\Sigma$ PAHs concentrations were observed to decrease for both the YRD (from 2,039.5 to 1,149.7  $\text{ngg}^{-1}$ ) and YHR (4222.7  $\text{ngg}^{-1}$  to 2,914.2  $\text{ngg}^{-1}$ ) samples. This is attributed to the turbulence of less contaminated, larger size sediments at higher turbulence energy, which skewed the compound concentration down-

ward and dilute the contaminants. Moreover, redistribution of PAHs to water column from the remobilized sediments might also contribute to the decrease of contaminant on particles under higher turbulence energy. The distribution of PAHs between solid and liquid phases showed that, for higher- $S_w$  PAHs (i.e., Ace and Flu), the conventional partition model exhibited generally less amount of PAHs than the measured data, especially for the YRD samples which had less  $f_{oc}$ . Accordingly, the model with additive consideration of surface properties was employed to better describe the sorption behavior of higher- $S_w$  PAHs. Based on this, an adjusted prediction model for describing the distribution of PAHs between solid and liquid phases in hydrodynamic systems were developed, and the prediction values displayed satisfying accordance with experimental data.

**Acknowledgements** The research was supported by the National Basic Research Program of China (973 Program, 2006CB403303) and the National Science Foundation for Distinguished Young Scholars (50625926). We gratefully acknowledge project 40701166 supported by National Natural Science Foundation of China.

#### References

- Ahrens MJ, Depree CV (2004) Inhomogeneous distribution of polycyclic aromatic hydrocarbons in different size and density fractions of contaminated sediment from Auckland Harbour, New Zealand: an opportunity for mitigation. *Mar Pollut Bull* 48:341–350
- Alkhatib E, Castor K (2000) Parameters influencing sediments resuspension and the link to sorption of inorganic compounds. *Environ Monit Assess* 65:531–546
- Alkhatib E, Weigand C (2002) Parameters affecting partitioning of 6 PCB congeners in natural sediments. *Environ Monit Assess* 78:1–17
- Allen-King RM, Grathwohl P, Ball WP (2002) New modeling paradigms for the sorption of hydrophobic organic chemicals to heterogeneous carbonaceous matter in soils, sediments, and rocks. *Adv Water Resour* 25:985–1016
- Chen JW, Peijnenburg W, Quan X, Chen S, Martens D, Schramm K-W, Kettrup A (2001) Is it possible to develop a QSPR model for direct photolysis half-lives of PAHs under irradiation of sunlight? *Environ Pollut* 114:137–143
- Chiou CT, McGroddy SE, Kile DE (1998) Partition characteristics of polycyclic aromatic hydrocarbons on soils and sediments. *Environ Sci Technol* 32:264–269
- Colombo JC, Cappelletti N, Lasci J, Migoya MC, Speranza E, Skorupka CN (2006) Sources, vertical fluxes, and equivalent toxicity of aromatic hydrocarbons in coastal sediments of the Rio de la Plata Estuary, Argentina. *Environ Sci Technol* 40:734–740
- DePinto J, Lick W, Paul J (1994) Transport and transformation of contaminants near the sediment-water interface. CRC Press/Lewis Publishers, Boca Raton, 33431
- de Vicente I, Cruz-Pizarro L, Rueda FJ (2010) Sediment resuspension in two adjacent shallow coastal lakes: controlling factors and consequences on phosphate dynamics. *Aquat Sci* 72:21–31
- Feng CL, Xia XH, Shen ZY, Zhou Z (2007a) Distribution and sources of polycyclic aromatic hydrocarbons in Wuhan section of the Yangtze River, China. *Environ Monit Assess* 133:447–458

- Feng JL, Yang ZF, Niu JF, Shen ZY (2007b) Remobilization of polycyclic aromatic hydrocarbons during the resuspension of Yangtze River sediments using a particle entrainment simulator. *Environ Pollut* 149:193–200
- Hedman JE, Tocca JS, Gunnarsson JS (2009) Remobilization of polychlorinated biphenyl from baltic sea sediment: comparing the roles of bioturbation and physical resuspension. *Environ Toxicol Chem* 28:2241–2249
- Joo JC, Shackelford CD, Reardon KF (2008) Sorption of nonpolar neutral organic compounds to humic acid-coated sands: contributions of organic and mineral components. *Chemosphere* 70:1290–1297
- Karickhoff S, Brown D, Scott T (1979) Sorption of hydrophobic pollutants on natural sediments. *Water Res* 13:241–248
- Kim HS, Weber WJ (2005) Optimizing contaminant desorption and bioavailability in dense slurry systems. 2. PAH bioavailability and rates of degradation. *Environ Sci Technol* 39:2274–2279
- Latimer JS, Davis WR, Keith DJ (1999) Mobilization of PAHS and PCBs from in-place contaminated marine resuspension events. *Estuar Coast Shelf Sci* 49:577–595
- Lee BC, Shimizu Y, Matsuda T, Matsui S (2005) Characterization of polycyclic aromatic hydrocarbons (PAHs) in different size fractions in deposited road particles (DRPs) from Lake Biwa area, Japan. *Environ Sci Technol* 39:7402–7409
- Long XX, Niu JF (2007) Estimation of gas-phase reaction rate constants of alkylnaphthalenes with chlorine, hydroxyl and nitrate radicals. *Chemosphere* 67:2028–2034
- Martino M, Turner A, Nimmo A, Millward GE (2002) Resuspension, reactivity and recycling of trace metals in the Mersey Estuary, UK. *Mar Chem* 77:171–186
- Niu JF, Yu G (2004) Molecular structural characteristics governing on biocatalytic oxidation of PAHs with hemoglobin. *Environ Toxicol Pharmacol* 18:39–45
- Niu JF, Chen JW, Martens D, Quan X, Yang FL, Kettrup A, Schramm K-W (2003) Photolysis of polycyclic aromatic hydrocarbons adsorbed on spruce (*Picea abies* (L.) Karst.) needles under sunlight irradiation. *Environ Pollut* 123:39–45
- Niu JF, Chen JW, Martens D, Henkelmann B, Quan X, Yang FL, Seidlitz HK, Schramm K-W (2004) The role of UV-B on the degradation of PCDD/Fs and PAHs sorbed on surfaces of spruce (*Picea abies* (L.) Karst.) needles. *Sci Total Environ* 322:231–241
- Niu JF, Sun P, Schramm K-W (2007) Photolysis of polycyclic aromatic hydrocarbons associated with fly ash particles under simulated sunlight irradiation. *J Photochem Photobiol A: Chem* 186:93–98
- Pignatello JJ, Lu YF, LeBoeuf EJ, Huang WL, Song JZ, Xing BS (2006) Nonlinear and competitive sorption of apolar compounds in black carbon-free natural organic materials. *J Environ Qual* 35:1049–1059
- Rockne KJ, Shor LM, Young LY, Taghon GL, Kosson DS (2002) Distributed sequestration and release of PAHs in weathered sediment: the role of sediment structure and organic carbon properties. *Environ Sci Technol* 36:2636–2644
- Saulnier I, Mucci A (2000) Trace metal remobilization following the resuspension of estuarine sediments: Saguenay Fjord, Canada. *Appl Geochem* 15:191–210
- Smit MPJ, Grotenhuis T, Bruning H, Rulkens WH (2010) Modeling desorption kinetics of a persistent organic pollutant from field aged sediment using a bi-disperse particle size distribution. *J Soils Sediments* 10:119–126
- Stout SA, Uhler AD, Emsbo-Mattingly SD (2004) Comparative evaluation of background anthropogenic hydrocarbons in surficial sediments from nine urban waterways. *Environ Sci Technol* 38:2987–2994
- Tao S, Cao HY, Liu WX, Li BG, Cao J, Xu FL, Wang XJ, Coveney RM, Shen WR, Qin BP, Sun R (2003) Fate modeling of phenanthrene with regional variation in Tianjin, China. *Environ Sci Technol* 37:2453–2459
- Tolosa I, de Mora S, Sheikholeslami MR, Villeneuve JP, Bartocci J, Cattini C (2004) Aliphatic and aromatic hydrocarbons in coastal Caspian Sea sediments. *Mar Pollut Bull* 48:44–60
- Troisi GM, Borjesson L (2005) Development of an immunoassay for the determination of polyaromatic hydrocarbons in plasma samples from oiled seabirds. *Environ Sci Technol* 39:3748–3755
- Urban SR, Correa AXR, Schettini CAF, Schwengel PR, Sperb RM, Radetski CM (2010) Physicochemical and ecotoxicological evaluation of estuarine water quality during a dredging operation. *J Soils Sediments* 10:65–76
- van der Heijden SA, Jonker MTO (2009) Evaluation of liposome-water partitioning for predicting bioaccumulation potential of hydrophobic organic chemicals. *Environ Sci Technol* 43:8854–8859
- Wang XC, Zhang YX, Chen RF (2001) Distribution and partitioning of polycyclic aromatic hydrocarbons (PAHs) in different size fractions in sediments from Boston Harbor, United States. *Mar Pollut Bull* 42:1139–1149
- Wang Z, Chen JW, Yang P, Qiao XL, Tian F (2007) Polycyclic aromatic hydrocarbons in Dalian soils: distribution and toxicity assessment. *J Environ Monit* 9:199–204
- Wang LL, Niu JF, Yang ZF, Shen ZY, Wang JY (2008) Effects of carbonate and organic matter on sorption and desorption behavior of polycyclic aromatic hydrocarbons in the sediments from Yangtze River. *J Hazard Mater* 154:811–817
- Wang LL, Shen ZY, Wang HY, Niu JF, Lian GX, Yang ZF (2009a) Distribution characteristics of phenanthrene in the water, suspended particles and sediments from Yangtze River under hydrodynamic conditions. *J Hazard Mater* 165:441–446
- Wang Y, Chen JW, Ge LK, Wang DG, Cai XY, Huang LP, Hao C (2009b) Experimental and theoretical studies on the photoinduced acute toxicity of a series of anthraquinone derivatives towards the water flea (*Daphnia magna*). *Dyes Pigment* 83:276–280
- Wang Y, Chen JW, Li F, Qin H, Qiao XL, Hao C (2009c) Modeling photoinduced toxicity of PAHs based on DFT-calculated descriptors. *Chemosphere* 76:999–1005
- Wang Z, Chen JW, Tian FL, Yang P, Qiao XL, Yao ZW (2010) Application of factor analysis with nonnegative constraints for source apportionment of soil polycyclic aromatic hydrocarbons (PAHs) in Liaoning, China. *Environ Forensics* 11:161–167
- Xing BS, Pignatello JJ, Gigliotti B (1996) Competitive sorption between atrazine and other organic compounds in soils and model sorbents. *Environ Sci Technol* 30:2432–2440
- Yang ZF, Feng JL, Niu JF, Shen ZY (2008) Release of polycyclic aromatic hydrocarbons from Yangtze River sediment cores during periods of simulated resuspension. *Environ Pollut* 155:366–374
- Yang ZF, Wang LL, Niu JF, Wang JY, Shen ZY (2009) Pollution assessment and source identifications of polycyclic aromatic hydrocarbons in sediments of the Yellow River Delta, a newly born wetland in China. *Environ Monit Assess* 158:561–571